Available online at www.sciencedirect.com

ScienceDirect

IFAC PapersOnline CONFERENCE PAPER ARCHIVE

IFAC PapersOnLine 55-6 (2022) 784–789

Model-based fault diagnosis of sliding gates electro-mechanical actuators transmission components with motor-side measurements

N. Valceschini *, **M. Mazzoleni** *, **F. Previdi** *

* *Department of Management, Information and Production engineering University of Bergamo, via Marconi 5, 24044 Dalmine (BG), Italy (e-mail: mirko.mazzoleni@unibg.it).*

Abstract: This paper presents a model-based fault detection and isolation scheme for the transmission components of Electro-Mechanical Actuators, applied to the actuation of sliding gates. The most important failures are investigated by a Failure Mode, Effects, and Criticality Analysis procedure. Following Failure Mode, Effects, and Criticality Analysis, the components selected for the development of the diagnostic algorithm are the nylon gear and pinion of the Electro-Mechanical Actuator, and the rack of the gate. The proposed diagnostic algorithm is able to isolate two out of the three types of faults. The overall procedure is validated by experimental results.

Keywords: FMECA; Fault detection; Fault isolation; Mechatronic systems

1. INTRODUCTION

Fault diagnosis is a relevant topic in the control community, concerned with the detection, isolation, identification and estimation of faults in dynamical systems, see Varga (2017). Although there is some overlap of terminology, we may distinguish between fault diagnosis and condition monitoring by considering the output type that those methods generally offer, see Mazzoleni et al. (2021). Fault diagnosis can be thought as mainly concerning a discrete (0/1) output, where the fault is detected or not, and eventually also which component is faulty (isolation) and the type, size and nature of the fault (identification). Condition monitoring may be though to pose more attention to produce a continuous indicator of a system's health state. Clearly, fault estimation (i.e. estimating the fault signal) can be interpreted as a kind of condition monitoring.

The present work is devoted to the development of a model-based fault detection and isolation algorithm for the transmission components of Electro-Mechanical Actuators (EMAs). Specifically, we mainly focus on the *diagnosis of gear wheels-like transmission components*. The proposed diagnostic scheme is applied to an experimental setup of EMAs that actuate sliding gates, where components, and their failures, have been selected using a Failures Mode, Effects and Criticality Analysis (FMECA). This applicative context is characterized by the employment of low-cost components. Thus, a major challenge is to detect faults without additional measurements.

The diagnosis of gears has been the focus of many studies in the literature, see (Randall, 2011, Chapter 5.4). Starting from Stewart (1977), who proposed a number of indicators for gearbox diagnostics based on Time Synchronous Averaging (TSA) and frequency analysis of a vibration signal, many other works followed with same diagnostic rationale, see Wang and Wong (2002); McFadden (1991). In Dowling (1993), the author introduces the use of Hilbert transformation to demodulate the vibration signal for a diagnostic purpose. The computation of a signal envelope by amplitude demodulation is one of the main techniques for detecting faults also in rolling bearings Sarda et al. (2021); Mazzoleni et al. (2021); Randall (2011). The aforementioned works consider the measurement of a vibration signal. Other methods for gear diagnosis make use of the so-called *transmission error* signal (Randall, 2011, Chapter 5.4), and then analyze its envelope in frequency domain, as in Du and Randall (1998). The transmission error represents the difference between the angular motion of a driven gear and that which it would have if the transmission were perfectly conjugate, that is constant speed out for constant speed in.

However, as in our application, it is not possible to compute this signal, since e.g. only a single encoder is present (usually motor-side), and it is not possible to add accelerometers due to the low-cost of the EMA equipments and envelope constraints, see Valceschini et al. (2021). The use of only motor-related measurements to perform diagnosis of EMAs has been previously investigated in the literature, especially for critical applications such as the aerospace industry Mazzoleni et al. (2019, 2017). Contrary to signal-based or knowledge-based methods for fault diagnosis, as in Mazzoleni et al. (2020, 2018), here we propose a *model-based fault detection and isolation* scheme for EMAs, that *relies only on common motor-side measurements* such as input voltage and motor speed.

The main contribution of this work lies in the *residual evaluation*: after the residual signal has been generated, it is processed by an envelope analysis to highlight the main fault frequencies that can raise when a component of the transmission chain is damaged. Then, a classifier is trained on features extracted on the frequency representation of

10.1016/j.ifacol.2022.07.222

the residual signal envelope. The designed classifier isolates two out of three faults, along with the healthy condition.

The paper is organized as follows. The experimental setup is discussed in Section 2. The FMECA procedure is described in Section 3. The test protocol and fault injections are presented in Section 4. The proposed model-based fault detection and isolation scheme is highlighted is Section 5. Section 6 presents the experimental result, while Section 7 concludes the paper.

2. EXPERIMENTAL SETUP

The system setup consists of a sliding gate actuated by a Direct Current (DC) motor with nominal voltage of $V_0 = 24\,\text{V}$. The control of the DC motor is made possible by a Pulse-Width Modulation (PWM) at 100 Hz of the input voltage signal. The gate moves by means of steel wheels on a steel rail. The motor is connected to the gate through a transmission that converts the DC motor rotation to a linear movement. The transmission is composed of: (i) a worm gear, (ii) a nylon gear, (iii) a shaft, (iv) a pinion and (v) a rack. We denote with the term Electro-Mechanical Actuator (EMA) the connection of the DC motor with the transmission elements (i)-(iv), while the rack is a component that belongs to the gate.

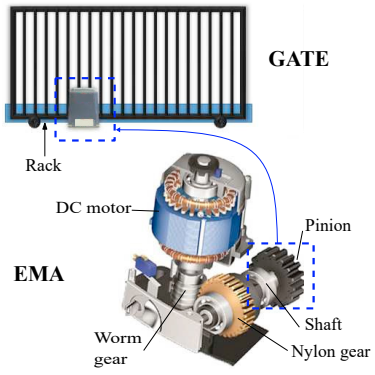

Fig. 1. Schematic representation of the overall system.

Figure 1 depicts how these elements are connected. In particular, the worm gear is welded to the rotor of the DC motor and it is coupled to the nylon gear with a primitive radius of $r = 28 \cdot 10^{-3}\,\text{m}$, that consists of 44 teeth, see Figure 2-(left). Since the rack is external to the EMA cover, a shaft connects the gear to the pinion, which in turn it is paired with the gate's rack. The rotation at the output of the EMA is transformed into linear motion by the pinon and the rack. The pinion is made of stainless steel and it has 14 teeth, see Figure 2-(right). An encoder measures the motor speed $\omega_M(t)$. The conversion from $\omega_M(t)$ to axial speed $v(t)$ can be made by the transmission ratio $\bar{\tau} = 1/47 \cdot r$. The motor resistance is $R = 0.7473\,\Omega$, and $k_t = k_e = K = 0.0696$ are the mechanical and electrical constants of the motor, respectively.

3. FAILURE MODE, EFFECTS, AND CRITICALITY ANALYSIS

In this work, we applied a Failure Mode, Effects, and Criticality Analysis (FMECA) to investigate the failures of the EMA and gate system. The FMECA is a reliability procedure that determines all potential failure modes of the various system's components, their effects, causes

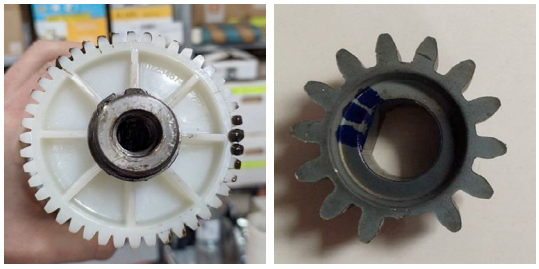

Fig. 2. Healthy nylon gear (left) and pinion (right).

and degree of criticality. The criticality analysis in the FMECA aids to define the so-called *criticality matrix*, used to classify the failures into a severity and frequency of occurrence levels, see Rausand (1994). This classification will be used to guide the selection of which failures should be considered by the proposed diagnostic algorithm.

The most occurring failures, appearing in years of maintenance reports, are: (1) rack with broken tooth; (2) pinion with broken tooth; (3) broken shaft; (4) broken nylon gear; (5) short circuit of the DC motor; (6) corrupted wheel. The resulting criticality matrix is depicted in Figure 3. By using this representation, each failure is allocated to a matrix cell, with assigned probability level (frequency of occurrence) and a severity level (criticality). The probability level is qualitatively defined as (A) probable, (B) remote, (C) extremely remote, (D) extremely improbable. The severity level is qualitatively described as indicating (I) catastrophic, (II) hazardous, (III) major and (IV) minor consequences, respectively. These qualitative levels should be understood as dependent on the specific system considered, see Mazzoleni et al. (2021); Rausand (1994); MIL-STD-1629A (1994).

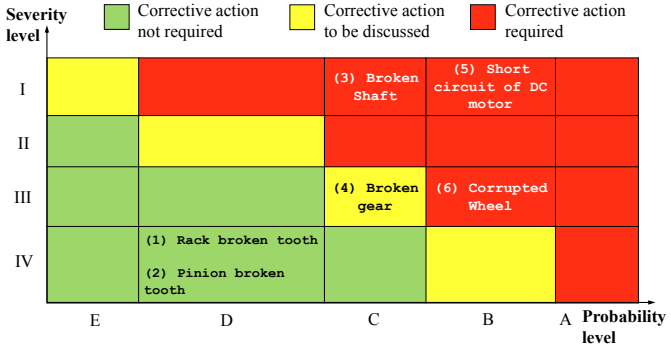

Fig. 3. Criticality matrix resulting from FMECA on the considered actuation system.

The `(3) Broken shaft` failure is classified in the cell (C-I) in the probability/severity table, since it occurs with extremely remote frequency and, moreover, it is a catastrophic phenomenon, because the shaft is disrupted into two pieces. Thus, in this condition, the EMA does not work. Another catastrophic event, that compromises the DC motor electronic, is the failure `(5) Short circuit of the DC motor`. Since this failure happens remotely, it was classified as (B-I).

Two failures that are not catastrophic, but still have major conseguences on the system, are: `(4) broken gear`, classified as (C-III) and `(6) corrupted wheel`, classified as (B-III). These failures do not stop the EMA operation, but

they make difficult the sliding of the gate. The operators common knowledge is that a broken nylon gear is the result of a natural notch on the gear that breaks through the entire gear radius. Due to this, the gear structure becomes weaker. After some movements, the less solid gear causes a misalignment that induces other cracks in the gear structure, leading to its disruption. Instead, the `(6) corrupted wheel` fault is due to the environmental corrosion that exhausts the wheel bearing. The failures that have minor consequences on the system are: `(1) Rack broken tooth` and `(2) Pinion broken tooth`, both classified as (D-IV). These are failures of the same type, i.e. a tooth breaks totally, on two different but connected components, see Figure 4. The EMA works properly with these failures.

The criticality matrix is used to assign a qualitative risk level for each failure, denoted by the cell color in Figure 3. Green and yellow cells contain the failures that do not require redesign of the actuation system. Instead, the red cells indicate the failures that can be prevented only by a system redesign, since those failures are too critical and/or too probable. The focus of the diagnostic algorithms will therefore be on the *failures that are not at the maximum risk level*, i.e. those in the green and yellow cells of the criticality matrix: `(1) Rack with broken tooth`; `(2) Pinion with broken tooth`; `(4) Broken nylon gear`.

4. FAULT INJECTION AND TEST PROTOCOL

4.1 Fault Injection

A fault injection procedure has been devised in order to collect measurements from a faulty system, considering the rack, pinion and nylon gear components. The rack and pinion faults were injected by removing a tooth using a vise, see Figure 4-(left) and 4-(right) respectively.

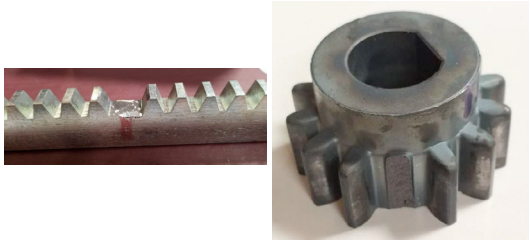

Fig. 4. Faulty rack (left) and pinion (right).

To reproduce the break of the nylon gear, we performed about one hundred gate movements (opening and closing) to break-in the component. After that, the fault is injected by carving perpendicularly the 80% of the total gear radius using a saw. The width of this notch is about 1 mm, see Figure 5-(left) where the area that contains the injected notch is highlighted in blue. In Figure 5-(left), it is possible to notice four mechanical housings, which aim is to hold the shaft joint. These are the most critical parts of the gear because they are subject to the force applied by the shaft through its joint. Thus, the fault is injected in this area. In this notched condition, the inner ring of the gear, i.e. the part that delimits the shaft slot, is still not broken. Thus, to induce its breakage, the carved gear is mounted on the EMA and about fifty openings and fifty closings are performed.

Figure 5-(right) represents the condition of the gear after the 100 movements. As depicted, the width of the natural notch is less than the width of the artificial one (highlighted in blue). It is important to remark that if the inner ring is completely broken by an artificial carve, e.g. with depth 100% of the gear radius, the structure would be too weak to perform any useful experiment.

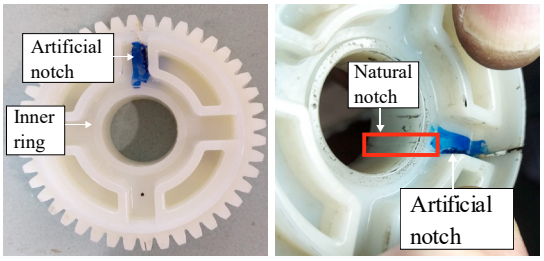

Fig. 5. Faulty nylon gear without breaking the inner ring (left); natural notch that breaks the inner ring (right).

4.2 Test protocol

The experimental protocol is composed of five different test plans: (i) healthy tests; (ii) gear fault tests; (iii) pinion fault tests; (iv) rack fault tests. All experiments share the same gate, binary and environment, but the fault injected is different. Only one fault at a time has been considered. In order to validate the diagnostic algorithm, the test protocol is performed twice with two different EMAs.

Each test plan consist in opening and closing gate movements, interspersed with a break of 7 seconds, in order to not overheat the motor. The motor is commanded in open-loop with trapezoidal voltage profiles, that define acceleration, constant speed, and deceleration phases. The rise and fall times of the acceleration and deceleration phases have been set to 1 s (the minimum settable acceleration/deceleration time). This choice is motivated by two ideas: the first one is that we wanted to perform movements that were stressful for the system (to enhance the fault detectability); the second reason regards the practical use of the gates, where the fastest opening and closing movements (but within laws regulations) are usually desirable.

The EMA hardware allows the acquisition of the following measurements with a sampling frequency of $f_s = 5000$ Hz:

(1) *motor speed* $\omega_M(t)$, measured by the motor encoder;
(2) *motor working phase* $p(t)$, showing which working phase the motor is currently performing (acceleration phase, constant velocity phase, deceleration phase);
(3) *motor current* $i(t)$, flowing in the DC motor coils;
(4) *motor voltage* $V(t)$, powering the motor.

5. MODEL-BASED FAULT DETECTION AND ISOLATION ALGORITHM

5.1 Modeling and identification

A mathematical model of the DC motor is presented in Figure 6, where: $F_L(t)$ is the load force opposing to the motor; L is the motor inductance; R is the motor resistance; D is the motor equivalent friction coefficient; J is the motor equivalent inertia; $\bar{\tau}$ is the transmission ratio; $K = k_t = k_e$ represents the motor mechanical and electrical constants; $V(t)$, $\hat{i}(t)$, $\hat{T}_M(t)$, $\hat{\omega}_M(t)$ $\hat{v}(t)$ are the

applied voltage input and simulated current, torque, motor rotational speed and load axial speed, respectively.

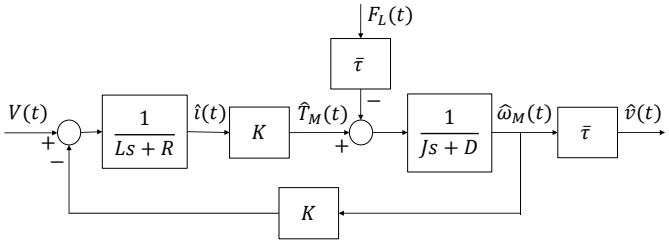

Fig. 6. Blocks scheme of the DC motor model.

It is interesting to notice that most of the parameters of this model are known from the motor datasheet or can be computed. The motor equivalent inertia can be expressed, in this rigid model, as $J = J_M + \bar{\tau}^2 \cdot m$, where J_M is the motor inertia and m is the weight of the gate. Both are known and correspond to $J_M = 3.5 \cdot 10^{-5}\,\mathrm{kg \cdot m}$ and $m = 608\,\mathrm{kg}$, respectively. To obtain the simplest possible model, we set $L = D = 0$.

From these hypotheses, it is possible to compute the complete transfer function from the input $V(t)$ to the output $\hat{v}(t)$ as:

$$\hat{W}(s) = \left(\hat{G}(s) - \hat{S}(s)\right) \cdot \bar{\tau} \tag{1a}$$

$$= \left(\frac{K}{JR \cdot s + K^2} - \frac{R\bar{\tau}}{JR \cdot s + K^2}\right) \cdot \bar{\tau}, \tag{1b}$$

where: $\hat{G}(s) = \frac{\Omega_M(s)}{V(s)}$ is the estimated transfer function from voltage $V(t)$ to motor speed $\omega_M(t)$; $\hat{S}(s) = \frac{\Omega_M(s)}{F_L(s)}$ is the estimated transfer function from the load force $F_L(t)$ to motor speed $\omega_M(t)$; s is the Laplace variable.

The force $F_L(t) = m \cdot g \cdot c_{\text{steel}}$ represents the sliding friction force of steel wheels on steel rail, with friction coefficient $c_{\text{steel}} = 3 \cdot 10^{-4}$ (see Astakhov (1966)), and g is the gravitational force. We assume $F(t)$ to be a constant force equal to $F_L(t) = \bar{F}_L = 0.19\,\mathrm{N}$.

The model (1) is thus completely known, but experimental data reveal the presence of an input-output delay. Thus, we identified a model of the form:

$$\hat{G}_d(s) = \frac{\mu}{T \cdot s + 1} \cdot e^{-s \cdot d} \tag{2}$$

where μ is the gain of $\hat{G}(s)$, T is the time constant of $\hat{G}(s)$ and d is the delay of the system [1]. A gray-box simulation error minimization is performed by minimizing the cost

$$J(d) = \frac{1}{N} \sum_{i=1}^{N} \left(v^c(t) - \hat{v}_d(t)\right)^2, \tag{3}$$

where the computed load axial speed $v^c(t)$ is obtained as $v^c(t) = \omega_M(t) \cdot \bar{\tau}$ (by considering the transmission as rigid), and $\hat{v}_d(t)$ is the simulated output of the model

$$\hat{W}_d(s) = \hat{G}_d(s) - \hat{S}(s). \tag{4}$$

[1] In the literature there exists a fault diagnosis method that detect faults through recursive parameter estimations, see Isermann (1993). This approach needs an input that excites the system sufficiently. Therefore, it is not applicable to this problem, because the available step input is not enough exciting to be used in black-box identification procedures.

The behaviour of the model in (4), for a opening gate movement not used for the identification, is depicted in Figure 8, where good simulation results can be observed.

5.2 Model-based fault detection and isolation scheme

Residual generation Figure 7 shows the proposed model-based fault detection strategy. The residual $r(t)$ is computed by an output-error based scheme, see (Isermann, 2006, Chapter 10), that compares the computed axial speed $v^c(t)$ (computed from the measure of $\omega_M(t)$), with the simulated output $\hat{v}_d(t)$ of model (4), given the same input $V(t)$:

$$r(t) = v^c(t) - \hat{v}_d(t). \tag{5}$$

The employment of the model in (4) allows to generate a residual signal that is able to *compensate for variations in speed*, even in the constant speed phase where speed oscillations are visible, see Figure 8. The disturbance $F_L(t)$ can not be decoupled from the residual since we only use one output measurement to perform fault detection. While there exists diagnostic schemes that try to reduce the effect of disturbances on the residuals, see (Ding, 2013, Chapter 7), in our application the effect of $F_L(t)$ on $v(t)$ is negligible since the gain of $\hat{S}(s)$ can be found to be $\mu_S = \frac{R \cdot \bar{\tau}^2}{K^2} \approx 5 \cdot 10^{-4}$, so that the signal $F_L(t)$, filtered through $\hat{S}(s)$, as an amplitude in the order of $10^{-5}\,\mathrm{m/s}$, which is negligible with respect to the amplitude of $v(t)$ (around $10^{-1}\,\mathrm{m/s}$).

Residual evaluation The proposed residual evaluation scheme, that is the main methodological contribution of this work, allows to *detect all three fault types* and to *isolate them in two categories*. The starting point is the observation that the mechanical transmission components of interest (e.g. rack, pinion and nylon gear) behave as a single component, since they are all connected together and also linked to the motor through the nylon gear. We thus expect that faults on the selected transmission components can be detected by using the same set of input/output measurements. Furthermore, the nylon gear and the pinion are basically gear wheels, where a tooth is removed by the fault injection procedure. As stated in the introduction, the envelope analysis of the transmission error can be employed to diagnose faults in gears.

The main idea of this work is to *apply the envelope analysis on the residual signal* $r(t)$ in (5). In this view, the signal $\hat{v}_d(t)$ can be effectively interpreted as the axial speed that one would have if the transmission were perfectly health and rigid, thus acting as a "virtual load encoder" signal. The true axial speed $v(t)$ will be affected by faults, but since the components are all linked together, we expect that also the computed axial speed $v^c(t)$ (or equivalently, the measured motor speed $\omega_M(t)$) will be affected.

The aim of the envelope analysis is to look for specific fault frequencies, as commonly done for rolling bearings Sarda et al. (2021); Randall (2011). Here, we look for the fault frequency f_{fault} that may appear on the shaft that connects the nylon gear to the steel pinion (which is then linked to the rack of the gate). Since, in our experiments, the rotational motor speed is known and it is about $\omega_M(t) = 4100\,\mathrm{rpm}$, the shaft rotational speed is

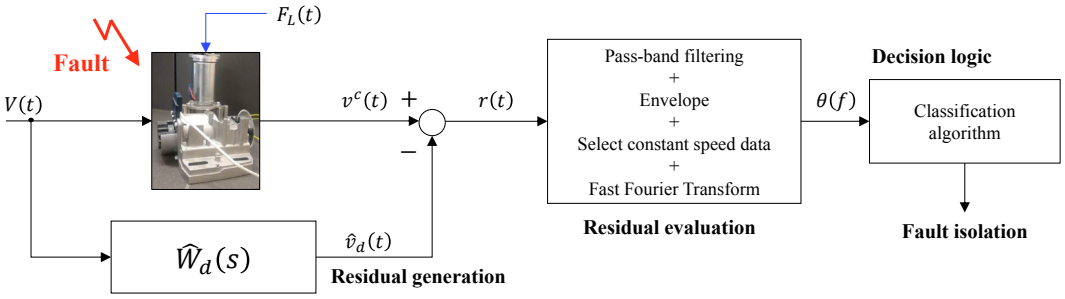

Fig. 7. Proposed model-based fault diagnosis scheme.

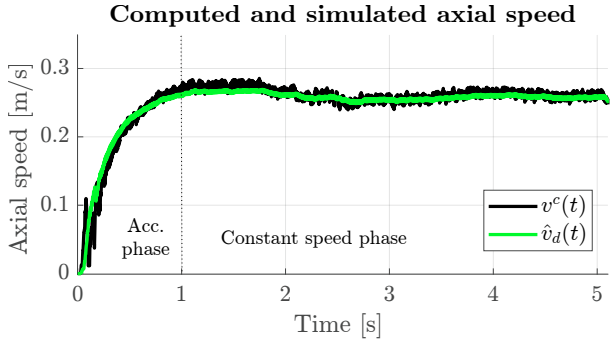

Fig. 8. Computed axial speed $v^c(t)$ from measurements and simulated axial speed $\hat{v}_d(t)$ by the model $\hat{W}_d(s)$.

$\frac{4100\,\text{rpm}}{44} \approx 93\,\text{rpm}$, where 44 is the ratio reduction from motor to shaft (i.e. the number of teeth of the nylon gear). Hence, the fault frequency of the components that are coupled to the shaft is about $f_{\text{fault}} = 1.55\,\text{Hz}$.

The envelope analysis of the residual signal $r(t)$ proceeds as follows. First, a bandpass filtering with bandwidth $[0.5, 10]\,\text{Hz}$ is employed to remove the continuous frequency and high-frequency noise. Then, the envelope of the filtered $r(t)$ signal (amplitude demodulation) is computed and constant phase speed data are retained for frequency analysis. The use of constant speed data allows to focus on a single fault frequency without employing advanced techniques like orders tracking[2], see (Randall, 2011, Chapter 3.6). The constant speed phase is always available in our application. A Fast Fourier Transform (FFT) of the envelope signal is then computed, and its modulus $\theta(f)$ analyzed for fault detection and isolation.

Finally, it is important to remark that the nylon gear fault and pinion fault (missing tooth) can be observed many times during the gate motion, but the faulty portion of the rack is visible only one time per gate movement (so that a frequency analysis is of limited utility in this case).

Decision logic A linear Support Vector Machines (SVM) classification algorithm is used to perform fault isolation. To this end, two features are computed from $\theta(f)$:

$$F_1 = \sum_{k=1}^{3} \theta(k \cdot f_{\text{fault}}); \quad F_2 = \sum_{k=1}^{3} \sum_{j=k\cdot f_{\text{fault}}\cdot 0.95}^{k\cdot f_{\text{fault}}\cdot 1.05} \theta(j). \quad (6)$$

[2] The importance of employing a model of the system lies in the fact that the residual signal in the constant speed phase, contrary to the axial speed $v(t)$, is much less subject to little variations due to external factors, so that the effects due to the faults can be better assessed.

The indicators in (6) extract the frequency amplitude at the first three harmonics of the fault frequency f_{fault} and the area in their neighbourhoods, respectively. This idea is inspired from Moster (2004), where those features are computed on the motor current signal.

The SVM algorithm classifies the features in (6) into three classes: health, pinion fault + nylon gear fault, rack fault. The nylon gear and pinion faults are difficult to isolate since these components are connected to the same shaft, so their rotation frequency is the same. Thus, a single "fault condition" has been considered for their isolation.

6. EXPERIMENTAL RESULTS

As stated in Section 4, we have at disposal two datasets, from two exemplars of the same EMA model. The first dataset is used to tune the parameters of the proposed procedure, such as the filtering band for the bandpass filter in the residual evaluation state. The training of the SVM classifier makes use of both the first and second datasets.

An example of FFT of the residual envelope $\theta(f)$ is depicted in Figure 9, where the fault frequency f_{fault} appear visible for the nylon gear and pinion fault. As expected, this frequency is not visible in the case of the rack fault, but a general increase of the frequency content is visible. Figure 10 depicts the 2D-plane composed of F_1 and F_2

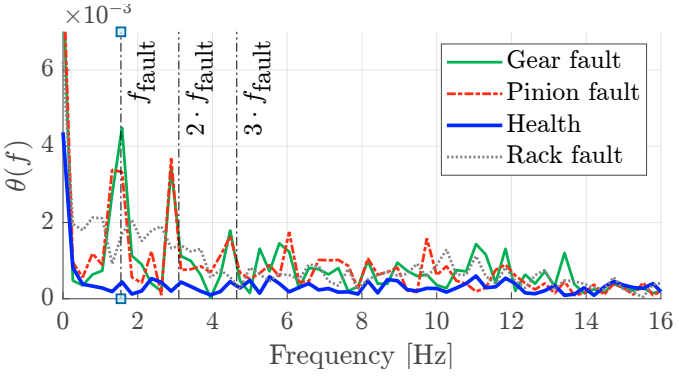

Fig. 9. Frequency analysis of the residual envelope.

features, computed using both datasets. The classifier performance have been evaluated by 10-fold cross-validation, resulting in an average cross-validation accuracy of 86.18% and variance of 0.33%. The classification boundaries, of the classifier *trained on all the data*, show a good capability of isolating the various kind of faulty conditions (considering the gear and pinion faults as a unique category), with

an accuracy of 96.15%[3]. Table 1 presents the confusion matrix of this classifier, using all the data.

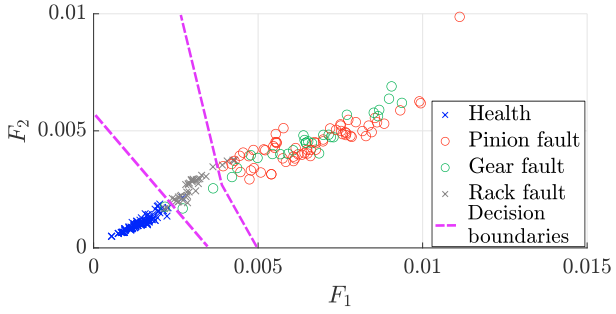

Fig. 10. Features plane and classification boundaries.

Table 1. Confusion matrix of the classifier trained on all the data.

		Real EMA state		
		Healthy	Pinon + gear faults	Rack fault
Estimated EMA state	Healthy	130	1	2
	Pinion + gear faults	0	89	4
	Rack fault	1	2	31

7. CONCLUSIONS

We presented a model-based fault detection and isolation algorithm for the transmission components of electro-mechanical actuators. The considered failures were chosen by a FMECA procedure, and specific faults were artificially injected or induced. The procedure employs only the input voltage and the motor speed, and it is based on the output speed residuals generated by a model of the DC motor. By adequately considering the type of faults to be diagnosed, we proposed a residual evaluation strategy based on the envelope analysis of the residual signal. Based on its frequency content, specific features have been extracted. An experimentally validated classifier trained on those features was shown to perform fault isolation of two out of three fault with good accuracy. Further research is devoted to the deployment of the algorithm on a micro-controller and its testing with different gate weights.

REFERENCES

Astakhov, P. (1966). *Resistance to motion of railway rolling stock.*

Ding, S. (2013). *Model-based fault diagnosis techniques: design schemes, algorithms, and tools, 2nd ed.* Springer Science & Business Media. doi:10.1007/978-1-4471-4799-2.

Dowling, M.J. (1993). Application of non-stationary analysis to machinery monitoring. In *1993 IEEE International Conference on Acoustics, Speech, and Signal Processing*, volume 1, 59–62. IEEE.

Du, S. and Randall, R. (1998). Encoder error analysis in gear transmission error measurement. *Proceedings of the Institution of Mechanical Engineers, Part C: Journal of Mechanical Engineering Science*, 212(4), 277–285.

[3] The model trained on all the data, its accuracy and confusion matrix should be considered as only a mean to highlight its decision boundaries and to represent the feature space. A more correct evaluation of the classifier's performance is given by the cross-validation routine.

Isermann, R. (1993). Fault diagnosis of machines via parameter estimation and knowledge processingâtutorial paper. *Automatica*, 29(4), 815–835. doi:https://doi.org/10.1016/0005-1098(93)90088-B.

Isermann, R. (2006). *Fault-Diagnosis Systems - An Introduction from Fault Detection to Fault Tolerance.* Springer-Verlag Berlin Heidelberg. doi:10.1007/3-540-30368-5.

Mazzoleni, M., Maccarana, Y., Previdi, F., Pispola, G., Nardi, M., Perni, F., and Toro, S. (2017). Development of a reliable electro-mechanical actuator for primary control surfaces in small aircrafts. In *2017 IEEE International Conference on Advanced Intelligent Mechatronics (AIM)*, 1142–1147. doi:10.1109/AIM.2017.8014172.

Mazzoleni, M., Scandella, M., Maccarana, Y., Previdi, F., Pispola, G., and Porzi, N. (2018). Condition monitoring of electro-mechanical actuators for aerospace using batch change detection algorithms. In *2018 IEEE Conference on Control Technology and Applications (CCTA)*, 1747–1752. doi:10.1109/CCTA.2018.8511334.

Mazzoleni, M., Scandella, M., Maurelli, L., and Previdi, F. (2020). Mechatronics applications of condition monitoring using a statistical change detection method. *IFAC-PapersOnLine*, 53(2), 92–97. doi:10.1016/j.ifacol.2020.12.100. 21th IFAC World Congress.

Mazzoleni, M., Previdi, F., Scandella, M., and Pispola, G. (2019). Experimental development of a health monitoring method for electro-mechanical actuators of flight control primary surfaces in more electric aircrafts. *IEEE Access*, 7, 153618–153634. doi:10.1109/ACCESS.2019.2948781.

Mazzoleni, M., Rito, G.D., and Previdi, F. (2021). *Electro-Mechanical Actuators for the More Electric Aircraft.* Springer International Publishing. doi:10.1007/978-3-030-61799-8.

McFadden, P. (1991). A technique for calculating the time domain averages of the vibration of the individual planet gears and the sun gear in an epicyclic gearbox. *Journal of Sound and vibration*, 144(1), 163–172.

MIL-STD-1629A (1994). Procedures for performing a failure mode, effects and criticality analysis. Technical report, USA Department of defense, Washington DC.

Moster, P. (2004). Gear fault detection and classification using learning machines. *Sound & vibration*, 38, 22–27.

Randall, R. (2011). *Vibration-based condition monitoring: industrial, aerospace and automotive applications.* John Wiley & Sons.

Rausand, Marvin adn HÃ¸yland, A. (1994). *System Reliability Theory: Models, Statistical Methods, and Applications, Second Edition.* Springer-Verlag London. doi:10.1002/9780470316900.

Sarda, K., Acernese, A., Russo, L., and Mazzoleni, M. (2021). A comparison of envelope and statistical analyses for bearing diagnosis in hot steel rolling mill lines. *47th Annual Conference of the IEEE Industrial Electronics Society (IECON).*

Stewart, R.M. (1977). Some useful data analysis techniques for gearbox diagnostic. *Proceedings of the Meeting on the Applications of Time Series Analysis.*

Valceschini, N., Mazzoleni, M., and Previdi, F. (2021). Inertial load classification of low-cost electro-mechanical systems under dataset shift with fast end of line testing. *Engineering Applications of Artificial Intelligence*, 105, 104446. doi:https://doi.org/10.1016/j.engappai.2021.104446.

Varga, A. (2017). Solving fault diagnosis problems. 84. doi:10.1007/978-3-319-51559-5.

Wang, W. and Wong, A.K. (2002). Autoregressive model-based gear fault diagnosis. *Journal Vibration and Acoustic*, 124(2), 172–179.